WATER RESOURCES RESEARCH, VOL. 29, NO. 8, PAGES 2861–2869, AUGUST 1993

A Fast and Exact Method for Multidimensional Gaussian Stochastic Simulations

C. R. DIETRICH

Division of Australian Environmental Sciences, Griffith University, Brisbane, Queensland, Australia

G. N. NEWSAM

Information Technology Division, Defense Science and Technology Organization, Salisbury, South Australia

To generate multidimensional Gaussian random fields over a regular sampling grid, hydrogeologists can call upon essentially two approaches. The first approach covers methods that are exact but computationally expensive, e.g., matrix factorization. The second covers methods that are approximate but that have only modest computational requirements, e.g., the spectral and turning bands methods. In this paper, we present a new approach that is both exact and computationally very efficient. The approach is based on embedding the random field correlation matrix R in a matrix S that has a circulant/block circulant structure. We then construct products of the square root $S^{1/2}$ with white noise random vectors. Appropriate subvectors of this product have correlation matrix R, and so are realizations of the desired random field. The only conditions that must be satisfied for the method to be valid are that (1) the mesh of the sampling grid be rectangular, (2) the correlation function be invariant under translation, and (3) the embedding matrix S be nonnegative definite. These conditions are mild and turn out to be satisfied in most practical hydrogeological problems. Implementation of the method requires only knowledge of the desired correlation function. Furthermore, if the sampling grid is a d-dimensional rectangular mesh containing n points in total and the correlation between points on opposite sides of the rectangle is vanishingly small, the computational requirements are only those of a fast Fourier transform (FFT) of a vector of dimension $2^d n$ per realization. Thus the cost of our approach is comparable with that of a spectral method also implemented using the FFT. In summary, the method is simple to understand, easy to implement, and is fast.

1. INTRODUCTION

The generation of realizations of spatially distributed Gaussian random fields, also termed stochastic simulations, has become increasingly useful in the geosciences; for example, they can be used to quantify uncertainty via the use of Monte Carlo simulations. Stochastic simulations have also provided insight into the convection and dispersion of a solute in groundwater systems [*Sposito et al.*, 1986; *Neuman*, 1990].

Stochastic simulations of the kind usually invoked in hydrogeology can be obtained in various ways. These include matrix decomposition techniques [*Davis*, 1987; *Fai Ma and Mills*, 1987], moving average [*Black and Freyberg*, 1990], nearest neighbor [*Bartlett*, 1955; *King and Smith*, 1988], spectral methods [*Shinozuka and Jan*, 1972; *Mejia and Rodriguez-Iturbe*, 1974; *Borgman et al.*, 1984], and turning bands [*Mantoglou and Wilson*, 1982; *Tompson et al.*, 1989].

An advantage of moving average and matrix factorization techniques is that both yield realizations whose ensemble mean in the limit displays exactly the desired correlation structure. Drawbacks of moving average and nearest neighbour methods are that the former does not extend to multidimensional problems, while the latter severely restricts the choice of the random field correlation structure. As for matrix factorization techniques, they are generally computationally very demanding. For example, on a two-dimensional rectangular grid Ω of p horizontal by q vertical points, current best algorithms for a triangularization of the random field's correlation matrix require at least $O(p^3q^2)$ floating point operations [*Dietrich*, 1993]. For these reasons, multidimensional stochastic simulations have most often been generated by the spectral and turning bands methods.

Realizations based on the spectral method are usually obtained by summing a finite cosine series whose coefficients have uniformly distributed random phases and amplitudes proportional to the spectral density function of the process. When this summation is calculated via the fast Fourier transform (FFT), a stochastic simulation generated by the spectral method will require $O(pq \log (pq))$ floating point operations. In the turning bands approach, multidimensional processes are generated from appropriately summed one-dimensional (or line) processes. Thus the costs are those of generating line simulations and appropriately projecting the resulting one-dimensional simulations onto the sampling grid. Therefore if l lines are used with each containing n intervals, the total costs will be $O(pql) + lc(n)$, where $c(n)$ is the cost of generating a single line realization. These figures indicate only the asymptotic dependency of the algorithms' costs on sample size. Nevertheless, they show that compared to exact factorization methods, the spectral and turning band methods have much more modest computational requirements.

This said, both methods have limitations. First, they are only asymptotically exact. In other words, the correlation structure of the ensemble of realizations is close to the structure required only if enough harmonics are used in the spectral method, or enough lines are generated in the turning bands approach. Moreover, as was shown in a recent study

Paper number 93WR01070.
0043-1397/93/93WR-01070$05.00

by *Black and Freyberg* [1990], use of the spectral method requires careful analysis and fine tuning of process parameters if spurious features in the resulting realizations are to be avoided. Furthermore, the method requires explicit knowledge of the Fourier transform of the correlation function (often termed the spectral density of the process).

As for the turning bands method, it can only be applied to processes with stationary and radially symmetric correlation functions, and it requires knowledge of the line structure for generation of the line realizations. For two-dimensional simulations, the line correlation is the solution to an Abel type integral equation [see *Mantoglou and Wilson*, 1982, p. 1383, equation (16)]. If no analytical inversion is known, the Abel integral may have to be solved numerically. Note, however, that the spectral density of the line process is very simply related to the radial spectral density function of the two-dimensional correlation function [*Mantoglou and Wilson*, 1982]. Thus solution of the Abel equation can be avoided if the radial spectral density is known and a spectral method is used to generate the line realizations. In three dimensions, the line correlation is simple to derive, but the issues of the appropriate number and distribution of lines through the unit sphere can be quite intricate [*Tompson et al.*, 1989].

Against this background, we present here a powerful new approach to the generation of multidimensional stationary Gaussian random fields. The approach is constructed as follows. Suppose that when sampled on the grid Ω, realizations of the random process have correlation matrix R which has block Toeplitz structure. Realizing that any block Toeplitz matrix R can be embedded in a larger block circulant matrix S, we use the standard eigendecomposition of a block circulant matrix in terms of the FFT to efficiently calculate a square root of S. Multiplication of a white noise vector by the square root $S^{1/2}$ of S now yields a random vector $e \sim \mathcal{N}(0, S)$. Since R is embedded exactly in S, a random vector distributed exactly as $\mathcal{N}(0, R)$ can now be got simply by extracting the appropriate subvector of e.

The only conditions required for this approach to be valid are (1) the mesh of the sampling grid is rectangular; (2) the correlation function is invariant under translation (i.e., the random field is stationary); and (3) the embedding matrix S is nonnegative definite. These assumptions are mild and turn out to be satisfied in most practical hydrogeological problems.

We stress that unlike the turning bands or spectral methods, our approach yields realizations whose ensemble displays exactly the desired field correlation structure. Furthermore, while our method uses the FFT for computational efficiency, knowledge of the Fourier transform of the correlation function is not necessary. If the sampling grid is a d-dimensional rectangular mesh containing n points in total, and the correlation between points on opposite sides of the rectangle is vanishingly small, computational requirements per realizations are only those of an FFT of a vector of dimension $2^d n$. Finally, as can be seen from the summary of the approach in two dimensions given in section 4, an additional feature of this new approach is the simplicity of its implementation.

The paper is organized as follows. In section 2, the approach is derived for one-dimensional problems. Implementation of the method when the correlation between points at either end of a one-dimensional grid is not vanishingly small is analyzed in section 3. In section 4, the approach is extended to multidimensional problems. In section 5, some numerical experiments for two-dimensional stochastic simulations are presented. Finally, some conclusions are drawn in section 6.

2. ONE-DIMENSIONAL SIMULATIONS

Consider a stationary line Gaussian process $Y(x)$ with zero mean and symmetric correlation function $r(x)$. A realization of $Y(x)$ on the grid of equispaced sampling points $\Omega = \{x_k = k\Delta x\}_{k=0}^{m}$ with mesh size Δx will have correlation matrix R with entries $R_{jk} = r(|x_j - x_k|)$, $0 \le j, k \le m$. Stationarity and equispacing ensure that the entries of R along each diagonal parallel to the main diagonal are identical; i.e., R is Toeplitz. As R is also symmetric, it is uniquely characterized by its first column

$$r = (\rho_0, \rho_1, \cdots, \rho_{m-1}, \rho_m)^T$$

where $\rho_k = r(k\Delta x)$, $k = 0, \cdots, m$, and the superscript T denotes transpose. Thus $R_{jk} = \rho_{|j-k|}$.

Consider now an embedding of R in the $2m \times 2m$ symmetric Toeplitz matrix S characterized by its first column s defined as follows:

$$s = (\rho_0, \rho_1, \cdots, \rho_{m-1}, \rho_m, \rho_{m-1}, \cdots, \rho_1)^T \qquad (1)$$

Observe that the first $m + 1$ elements in s are exactly the $m + 1$ entries in r so that R is exactly embedded in S. Also, the entries in s are symmetrically arranged on both sides of ρ_m except for the first entry ρ_0. Thus it is straightforward to verify that S is circulant, i.e., that its successive columns are obtained by successive cyclic permutations of the first column. This implies that S has the eigenvalue decomposition [*Barnett*, 1990, p. 252]

$$S = \frac{1}{2m} W\Lambda W^*$$

Here W is the one-dimensional discrete Fourier transform matrix of dimension $2m$ with entries $w_{pq} = \exp(2\pi ipq/2m)$ for $0 \le p, q \le 2m - 1$ and $i^2 = -1$, and W^* is the conjugate transpose of W. The eigenvalues in the diagonal matrix Λ form the vector $\bar{s} = Ws$. Because of the symmetry in the entries in s, the entries $\bar{s}_j$ of $\bar{s}$ can also be written as

$$\bar{s}_j = \rho_0 + \rho_m \cos(\pi j) + 2\sum_{k=1}^{m-1} \rho_k \cos(\pi jk/m) \qquad (2)$$

$$j = 0, \cdots, m$$

Now, if all entries $\bar{s}_j$ are nonnegative, S can be decomposed as

$$S = \frac{1}{2m} W\Lambda^{1/2}(W\Lambda^{1/2})^*$$

In this respect, if the entries $\bar{s}_j$ are nonnegative so that S is a nonnegative definite matrix, then we shall say that R has a nonnegative definite circulant embedding, or nonnegative embedding, for short.

Assuming for the moment that R does have a nonnegative embedding, let ε be a random complex variable of the form

$\varepsilon = \varepsilon_1 + i\varepsilon_2$, where ε_1 and ε_2 are real, normal, zero mean random vectors of dimension $2m$ with $E[\varepsilon_j \varepsilon_k^T] = \delta_{jk} I$ for $j, k = 1, 2$. Here E denotes the expectation, I is the $2m \times 2m$ identity matrix, and δ_{jk} is the Kronecker operator. Then the real and imaginary parts of the vector $W(\Lambda/2m)^{1/2}\varepsilon$ form two independent real random variables that are both distributed as $\mathcal{N}(0, S)$ (see Appendix A). Thus since the submatrix formed by the top left $(m + 1) \times (m + 1)$ block of S is just R, the first $m + 1$ entries of the real and imaginary parts of $W(\Lambda/2m)^{1/2}\varepsilon$ are independent of each other and are each distributed as $\mathcal{N}(0, R)$. Hence they are two independent realizations of $Y(x)$ with exactly the required correlation structure on the sampling points in Ω.

As the approach remains essentially unchanged for simulations of higher dimensions, a summary of the algorithm and discussion of computational costs are postponed until section 4 where the approach is presented for two-dimensional simulations.

Clearly, the approach fails if $\bar{s}$ has a strictly negative component. Therefore in the next section, practical criteria that ensure nonnegative embeddings are provided.

3. Nonnegative Embeddings

Consider the sequence of correlation samples $\{\rho_k = r(k\Delta x)\}_{k=0}^{\infty}$. As is shown in Appendix B, the application of standard results from sampling theory ensures that the sum

$$\rho_0 + 2\sum_{k=1}^{\infty} \rho_k \cos(\pi jk/m) \tag{3}$$

is nonnegative for any value of j. Now assume that the correlation function $r(x)$ is such that $\rho_k = 0$ if $k \geq m$. Then from (2) and (3) we have immediately

$$\bar{s}_j = \rho_0 + 2\sum_{k=1}^{m-1} \rho_k \cos(\pi jk/m) \geq 0 \qquad j = 0, \cdots, m$$

In other words, our method can always be implemented if the correlation function is zero beyond a certain length l and the grid $\Omega = \{x_k = k\Delta x\}_{k=0}^{m}$ samples this correlation function over the whole interval $[0, l]$. Correlation functions $r(x)$ with the property $r(x) = 0$ when $x \geq l$ are said to have bounded support on $[0, l]$. Well-known examples are the spherical correlation

$$r(x) = 1 - \frac{3}{2}\frac{|x|}{l} + \frac{1}{2}\left(\frac{|x|}{l}\right)^3 \qquad 0 \leq x \leq l,$$

$$r(x) = 0 \qquad \text{otherwise.}$$

and power model [*Mardia and Watkins*, 1989]

$$r(x) = \left(1 - \frac{|x|}{l}\right)^{\gamma} \qquad \gamma \geq 1 \qquad 0 \leq x \leq l,$$

$$r(x) = 0 \qquad \text{otherwise.}$$

For correlation functions with infinite support, such as the Gaussian model $r(x) = e^{-(x/l)^2}$, our approach can be applied by simply increasing the number of sampling points until the correlation between the first point x_0 and the last point x_m is vanishingly small. Because simulations are usually sought over an interval $[0, L]$ such that the length scale l of the process is only a small fraction of the interval size L, the standard correlation functions used in hydrogeological problems will usually have decayed to quite small values for $x \approx L$. Therefore a sampling grid on the interval $[0, L]$ will usually have sufficient breadth to ensure the nonnegativity of the components in $\bar{s}$; if they are not then in principle nonnegativity can always be eventually obtained by simply increasing L. In practice, for large L nonnegative components may still appear, but they are usually smaller than machine precision. Thus they can be set to zero without changing in any significant way the accuracy of the overall stochastic simulations.

Another point to keep in mind is that we have so far only considered correlation functions with no nugget effect. If a nugget effect is included in the stochastic simulations, all components in $\bar{s}$ will be increased by an amount equal to the size of the effect. Thus the occurrence of negative components will be significantly reduced, as shown in numerical experiments reported in section 5.

Rigorous results on these issues, such as bounds on the number of sampling points needed to ensure nonnegative embeddings, can be found in the work by C. R. Dietrich and G. N. Newsam (Fast and exact generation of stationary Gaussian processes via circulant embeddings of the correlation matrix, submitted to *SIAM Journal on Scientific Computing*, 1992; hereinafter referred to as Dietrich and Newsam, submitted manuscript, 1992). In particular, it is shown there that, in one dimension, embeddings of correlation functions that are convex and nonincreasing (e.g., the exponential decay $r(x) = e^{-|x|/l}$) will always be nonnegative for any correlation length and any equispaced grid Ω of sampling points. This is also shown to be true for some nonconvex, nonstrictly decreasing correlation functions, such as the hole effect $r(x) = (1 - |x|/l)e^{-|x|/l}$.

4. Higher-Dimensional Simulations

Two-Dimensional Simulations

We first look at simulations in two dimensions. Let Δx and Δy be constants denoting respectively, the horizontal and vertical mesh sizes in a rectangular two-dimensional grid Ω formed by the points $\mathbf{x}_{pq} = (x_p, y_q)$, where $x_p = p\Delta x$ and $y_q = q\Delta y$ with $0 \leq p \leq m$ and $0 \leq q \leq n$. Stationarity and equispacing now ensure that the correlation matrix R is block Toeplitz and block symmetric, with each block being itself Toeplitz and symmetric [*Zimmerman*, 1989]. Therefore R is uniquely characterized by its first block column

$$R_0 = (R_{00}, R_{01}, \cdots, R_{0n})^T$$

with each block R_{0i}, $i = 0, \cdots, n$ being of dimension $m + 1$. Following exactly the argument developed for the one-dimensional case, each block R_{0i} can be embedded in a symmetric and circulant matrix S_{0i} of dimension $2m$. With this, let S denote the $4mn \times 4mn$ block circulant matrix with first block column S_0 equal to

$$S_0 = (S_{00}, S_{01}, \cdots, S_{0(n-1)}, S_{0n}, S_{0(n-1)}, \cdots, S_{01})^T \tag{4}$$

Observe that as in (1), the block entries in S_0 are symmetrically arranged on both sides of S_{0n} except for the presence

of S_{00} as the first block entry. As in the one-dimensional case, let s denote the first column of S.

Clearly, S is uniquely defined by (4) and R is embedded in S. Let W be the two-dimensional discrete Fourier transform matrix whose entries are defined by $w_{puqv} = \exp((2\pi i(pu/2m + qv/2n))$, with $0 \le p, u \le 2m - 1$ and $0 \le q, v \le 2n - 1$. Then S has the eigenvalue decomposition $S = (1/4mn)W\Lambda W^*$, with the eigenvalues in the diagonal matrix Λ being the entries in the vector $\bar{s} = Ws$. Thus if all components in $\bar{s}$ are nonnegative, the decomposition $S = (1/4mn)W\Lambda^{1/2}(W\Lambda^{1/2})^*$ is possible, and the argument given in section 2 carries through. In particular, if $\varepsilon = \varepsilon_1 + i\varepsilon_2$ is a random complex vector of dimensional $4mn$ with ε_1 and ε_2 being real, zero mean, normal random variables such that $E[\varepsilon_i \varepsilon_j^T] = \delta_{ij} I$, the real and imaginary parts of the vector $e = W\bar{e}$ with $\bar{e} = (\Lambda/4mn)^{1/2}\varepsilon$ yield two real and independent random vectors that are both $\mathcal{N}(0, S)$.

As R is embedded in S, it remains to extract from e two $\mathcal{N}(0, R)$ vectors that are realizations of Y. To do this, it is helpful to digress slightly and consider the actual implementation of the two-dimensional discrete Fourier transform. As is shown by *Press et al.* [1986, pp. 450–452], the transform is easy to visualize once the vectors e and $\bar{e}$ are rearranged in the form of two dimensional arrays E and $\bar{E}$. The array E is obtained from e as follows: the first column of E consists of the first $2m$ entries of e, the second column of E takes the next $2m$ entries of e, and so on. The same applies in forming $\bar{E}$ from $\bar{e}$. Conversely, if E or $\bar{E}$ are known, the inverse procedure yields e or $\bar{e}$ uniquely. In this framework the relationship $e = W\bar{e}$ takes the form

$$E(p, q) = \sum_{u=0}^{2m-1} \sum_{v=0}^{2n-1} \exp(2\pi i(pu/2m + qv/2n))\bar{E}(u, v) \tag{5}$$

This indicates that the two realizations of Y are simply the real and imaginary parts of the first $m + 1$ row entries in the first $n + 1$ columns of E.

To summarize our approach, provided the embedding of R in the block circulant matrix S with circulant blocks S_{0i} results in the components of the two-dimensional discrete Fourier transform $\bar{s}$ of the vector s characterizing S being nonnegative, our method for two-dimensional stochastic simulations is as follows.

1. Construct the first column s of the circulant matrix S defined via its first block column as in (4).
2. Compute the two-dimensional FFT $\bar{s}$ of the vector s and form the vector $(\bar{s}/4mn)^{1/2}$.
3. Generate a vector $\varepsilon = \varepsilon_1 + i\varepsilon_2$ of dimension $4mn$ with ε_1 and ε_2 being two $\mathcal{N}(0, I)$ vectors of independent real random variables.
4. Multiply each entry of ε by the corresponding entry of $(\bar{s}/4mn)^{1/2}$, yielding the vector $\bar{e}$.
5. Compute the two-dimensional FFT e of the vector $\bar{e}$. The real and imaginary part of the first $m + 1$ row entries in the first $n + 1$ columns of the associated array E now yield two independent realizations of Y over the grid Ω.
6. Go to step 3.

An important point to note is that despite the use of complex notation, our approach does not require the use of complex arithmetic. For example, the generation of the complex random vector ε simply requires two real independent vectors $\varepsilon_1 \sim \mathcal{N}(0, I)$ and $\varepsilon_2 \sim \mathcal{N}(0, I)$ stored in two separate real arrays of dimension $4mn$ as inputs to the FFT routine. Complex number notation has only been invoked here because it simplifies exposition of the approach, and because the FFT algorithm, which is the cornerstone of the approach, takes complex vectors as its natural inputs [*Press et al.*, 1986].

The computational requirements of the methods are as follows. The products Ws and We can be computed by the FFT. This means that the computation of realizations of $Y(x)$ will be dominated by one FFT of dimension $4mn$ to first form $\bar{s} = Ws$ and, thereafter, one FFT of dimension $4mn$ for each pair of realizations. This represents an overall cost of $O(4mn \log_2 (4mn))$ floating point operations per realization, with $O(4mn)$ storage.

As in one-dimension, our approach fails if any component in $\bar{s}$ is strictly negative. However, the results in section 3 can easily be extended to show that if the correlation between points that are sufficiently far apart (in particular, between points on opposite sides of the grid Ω) is zero then the components of $\bar{s}$ are always nonnegative. That is, if the correlation between two points $\mathbf{x} = (x_1, x_2)$ and $\mathbf{y} = (y_1, y_2)$ is zero if $|x_1 - x_2| \ge m\Delta x$ or $|y_1 - y_2| \ge n\Delta y$ then the embedding will be nonnegative. This implies for example that correlation functions with bounded support $[0, l_1] \times [0, l_2]$ (where l_1 and l_2 are the length scales in the horizontal and vertical dimensions) will have nonnegative embeddings as long as $l_1 \le |x_0 - x_m|$ and $l_2 \le |y_0 - y_n|$. This applies in particular to the isotropic spherical and power models mentioned in the previous section. The existence of nonnegative embeddings for two-dimensional correlation functions withy bounded support appears to have been first noted by *Woods* [1972] in an examination of Markov random fields.

We also note that since, as mentioned in section 3, the correlation model $e^{-|x|/l}$ yields nonnegative embeddings for any equispaced sampling grid Ω in one dimension, a simple tensor product argument shows that the separable, anisotropic correlation function in two dimensions

$$r(\mathbf{x}, \mathbf{y}) = e^{-(|x_2 - x_1|/l_1 + |y_2 - y_1|/l_2)} \tag{6}$$

$$\mathbf{x} = (x_1, x_2), \mathbf{y} = (y_1, y_2) \in R^2$$

will always result in nonnegative components in $\bar{s}$.

For correlation functions that are not identically zero beyond some length scale, the sampling grid can be increased until the correlation between points on opposite sides of the grid is essentially zero. Also, if simulations are required over a grid that is regularly meshed but has an irregular boundary, it is always possible to embed the irregularly shaped grid in a larger rectangular grid Ω and apply the approach on Ω.

Three-Dimensional Simulations

The extension of the algorithm to three-dimensional problems is straightforward once it is realized that over a three-dimensional rectangular and regularly meshed sampling grid Ω, the correlation matrix of the process will be block symmetric and block Toeplitz with each block having all the properties of the correlation matrix in two dimensions. In other words, each block of R will itself be block Toeplitz and block symmetric with each subblock Toeplitz and symmetric. Consequently, the strategy of embedding R into an appropriate circulant matrix S remains valid, and the

summary of the two-dimensional algorithm carries across to three dimensions with the two-dimensional FFT being replaced by the three-dimensional FFT. Thus if Ω is rectangular and the correlation between points on opposite sides of Ω is vanishingly small, computational requirements are now $O(\Pi_{i=1}^{3}\ 2m_i\ \log_i\ (2m_i))$ floating point operations where $m_i + 1$ is the number of mesh points on each of the three sides of Ω.

In conclusion, the algorithm presented here has a remarkably simple form that can be applied equally easily in any dimension. In general, however, the approach is valid only if the correlation between opposite sides of the sampling grid Ω is zero. If this is not the case, negative components in $\bar{s}$ may emerge. In such a case modelers have several alternatives. The first is simply to set any negative components to zero and so generate realizations whose correlation only approximates that required. If the negative components are small, any error incurred is likely to be well within the errors in the modeling process as a whole and so can be ignored. A variation on this approach is to introduce a small nugget effect: this raise all components by the same amount and can be increased until all negative components have been made positive.

If approximations are not acceptable, one can ensure nonnegativity by either decreasing the length scale of the correlation function or increasing the size of the sampling grid Ω, so that eventually the correlation between opposite sides of Ω is essentially zero. Either alternative will always work eventually, but at a price: reducing the length scale will reduce the detail of realizations seen on the fixed grid, while increasing Ω will increase computational requirements. Indeed, a doubling in the size of Ω will multiply the computational costs of our approach by roughly a factor of 4 in two dimensions and 8 in three dimensions. Fortunately, in most hydrological problems the grid Ω is sufficiently large compared to the length scale so that points on opposite sides of the sampling grid are essentially uncorrelated.

Finally, we note that if the sample grid is not rectangular, our method can still be implemented by simply adding nodes to the sampling domain until it is rectangular.

5. Numerical Experiments

As was noted earlier, there are correlation functions, e.g., (6), for which our approach is valid for any correlation length and for any rectangularly meshed and multidimensional sampling grid Ω. Furthermore, for correlation functions with bounded support, our approach is always valid provided the correlation length in any coordinate direction is smaller than the associated side length of Ω. The latter holds true for most geohydrological problems as the size of the geohydrological formation over which stochastic simulations are sought is usually several times larger than the correlation length scale.

For correlation functions with infinite support, negative components in $\bar{s}$ may occur if the correlation function does not decay sufficiently quickly over the whole extent of Ω. Although it is possible to provide further analytical results for some correlation functions that will ensure nonnegative embeddings (see Dietrich and Newsam, submitted manuscript, 1992), we shall content ourselves here with reporting numerical experiments performed with correlation functions often used in practical hydrogeological problems. These experiments show that in practical situations nonnegative embeddings can still be found even for correlation functions with infinite support.

First, for convenience we assume that Ω is square and has a square mesh with spacing $\Delta x = \Delta y = \Delta$, so that $m = n$. We also assume that the correlation function is isotropic, so the correlation $r(|\mathbf{x} - \mathbf{y}|)$ between any two points $\mathbf{x}$ and $\mathbf{y}$ is a function only of the distance between $\mathbf{x}$ and $\mathbf{y}$. Thus the length scale l is the same in the vertical and horizontal directions. Therefore the correlation between corner points of Ω in either the x or y direction is $r(\alpha)$ where

$$\alpha = m\Delta/l$$

Note that α represents the ratio between the width of Ω and the length scale l.

The idea now is to compute the smallest element in $\bar{s}$ for a range of values of m and α. For a given m and α let $\beta(m, \alpha)$ denote the smallest element in $\bar{s}$, namely,

$$\beta(m, \alpha) = \min_j \{\bar{s}_j\}$$

Because most correlation functions used in practice decay rapidly beyond their correlation length, we expect that for a fixed value of m, $\beta(m, \alpha)$ will be nonnegative if α is sufficiently large. Conversely, if α is small, $\beta(m, \alpha)$ may be strictly negative. Similarly, for a fixed value of α, $\beta(m, \alpha)$ will be nonnegative if m is sufficiently large and, conversely, if m is small, $\beta(m, \alpha)$ may be strictly negative. It is worth noting here that for large m, $\beta(m, \alpha)$ will generally be of very small absolute value regardless of its sign. This effect will be more pronounced for smooth correlation functions as the associated correlation matrix will generally have extremely small eigenvalues [*Newsam*, 1988].

To illustrate these issues, we shall consider the following three correlation functions:

Exponential

$$r(|\mathbf{x}|) = e^{-|\mathbf{x}|/l}$$

Gaussian

$$r(|\mathbf{x}|) = e^{-(|\mathbf{x}|/l)^2}$$

and Whittle

$$r(|\mathbf{x}|) = (|\mathbf{x}|/l)K_1(|\mathbf{x}|/l)$$

where K_1 is the second kind modified Bessel function of order one. As was observed by *Whittle* [1954], the Whittle correlation is a natural correlation in two dimensions as it is the correlation of a stochastic process obtained from Laplace's equation with a white noise forcing term. In other words, the Whittle correlation "may be regarded as the elementary correlation in two dimensions, similar to the exponential model in one dimension" [*Jones*, 1989, p. 86]. To compare the rate of decay of these three correlation functions the reader may turn to Figure 1 where each function is plotted over [0, 5] with $l = 1$. Note that these three models have infinite support. Correlation functions with finite support such as the spherical or power model were not considered in these experiments, as it has already been shown that the required embedding is always nonnegative definite whenever the sampling grid covers the correlation length scale.

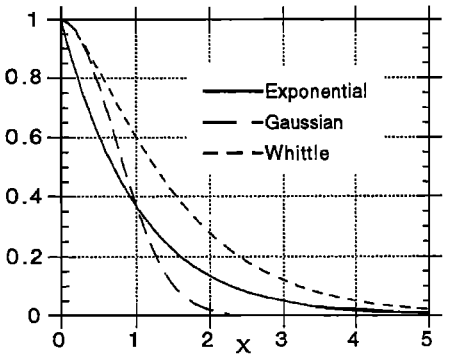

Fig. 1. Decay of the exponential, Gaussian, and Whittle correlation functions away from the origin.

The first set of experiments computed the value of $\beta(m, \alpha)$ for the above three correlation functions for a fixed value $m = 20$ and for α varying from 0 to 5 in equispaced steps of length $\Delta\alpha = 0.1$. The results are shown in Figure 2. The first point to note is that $\beta(m, \alpha)$ is equal to zero when $\alpha = 0$. Indeed, this feature holds true for any correlation function and any value of m since $\alpha = 0$ results in the matrix S having all entries equal to 1. Its eigenvalues are thus all zero except for one equal to the sum of its first column entries.

The value of α for which $\beta(20, \alpha)$ became strictly positive was 3.1 for the exponential correlation. For the Gaussian and Whittle correlations, $\beta(20, \alpha)$ remained negative over [0, 5] although, as can be seen in Figure 2, it increasingly approaches zero once α is greater than 1.

The next step of experiments involved the computation $\beta(m, \alpha)$ with both m and α varying. For this, we chose to vary m between 10 and 80 in steps of 10. As for α, it was sampled at equispaced steps of length $\Delta\alpha = 0.2$ between 2 and 5 for the exponential and Gaussian model. For the Whittle model, α was sampled between 4 and 8 as the Whittle correlation function has a much slower rate of decay than the others (see Figure 1). For the three models, results are plotted in Figure 3. Furthermore, the values of α for which β first becomes positive are given in the columns labeled "no nugget" of Table 1.

Table 1 and Figure 3 are guides to the extent to which the tail of the correlation has to be sampled in order to ensure nonnegativity of all components in $\tilde{s}$. For example, the exponential model with $m = 50$ requires $\alpha \geq 3.9$ for this to happen. In other words, the width of the sampling grid Ω has

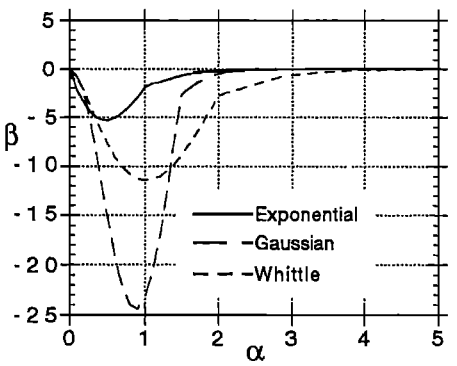

Fig. 2. Values of $\beta(m, \alpha)$ with fixed $m = 20$ with a varying.

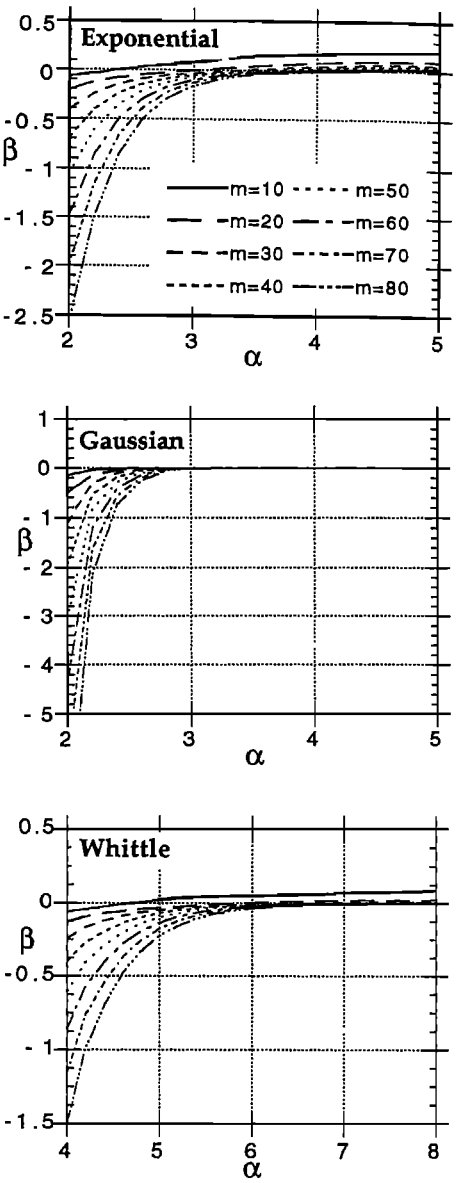

Fig. 3. Values of $\beta(m, \alpha)$ for both m and α varying and no nugget effect. The legend displayed for the exponential is the same for the Gaussian and Whittle models.

to be at least $3.9l$. For the Gaussian model, this width has to be at least $5.5l$. However, the associated value of β is extremely small. Indeed, for $\alpha \geq 4$ all values of $\beta(50, \alpha)$ are in absolute value smaller than 10^{-6}. They can thus be set to zero and the algorithm applied without introducing any significant errors. For the Whittle correlation function, the grid width has to be greater than $7.6l$. This rather large value is not surprising given the slow decay of the Whittle correlation function compared to the others (see Figure 1).

So far, we have assumed a correlation function that is continuous at the origin, i.e., is without a nugget effect [*Journel and Huijbregts*, 1978]. If a nugget effect is included in the simulations, the correlation matrix will be of the form $\theta_0 I + \theta_1 R$, where $\theta_i \geq 0$, $\theta_0 + \theta_1 = 1$ and I denotes the identity matrix. Obviously, the associated circulant matrix will now be $\theta_0 I + \theta_1 S$. Because the entries in $\tilde{s}$ are the eigenvalues of S, the effect of the nugget effect is to increase all entries in $\theta_1 \tilde{s}$ by the amount θ_0. This means that very

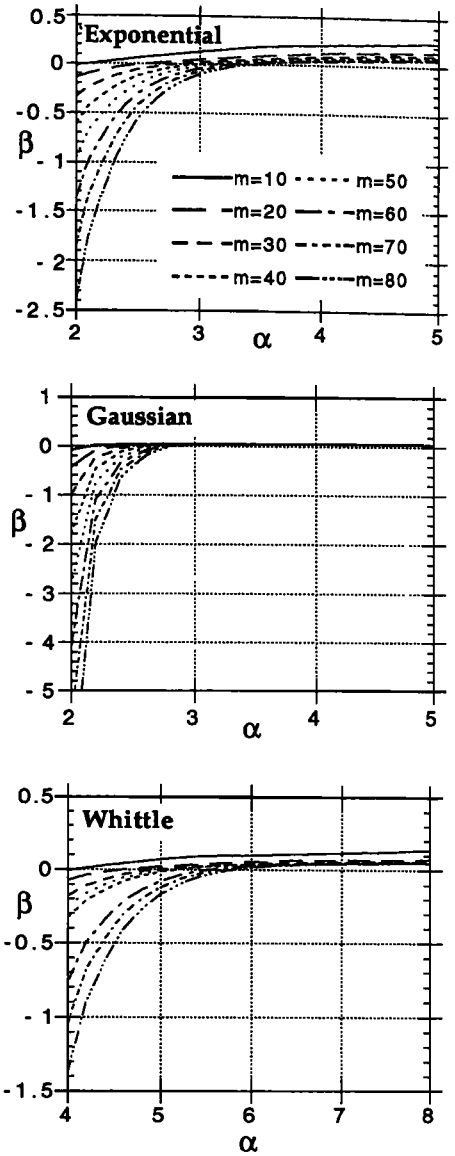

Fig. 4. Values of $\beta(m, \alpha)$ for both m and α varying and a 5% nugget effect. The legend displayed for the exponential is the same for the Gaussian and Whittle models.

small negative values of β will be made positive when a nugget effect of larger magnitude is included. For example, the negative values of β for the Gaussian model are all of very small magnitude. They will therefore be filtered out if a nugget effect of moderate magnitude is invoked.

To illustrate the changes introduced by a nugget effect, the above tests were repeated with $\theta_0 = 0.05$ and $\theta_1 = 0.95$. The results corresponding to Figure 3 are in Figure 4 with Table 1 providing values of α for which β is zero. Note in Table 1 that the number of length scales over which the correlation has to be sampled has been significantly reduced for all three correlation models.

For the exponential and Gaussian models the above experiments show that all components in $\bar{s}$ will be nonnegative if the correlation length scale l is a sufficiently small fraction of the sampling grid's width. In particular, for a small nugget effect of about 5% the correlation length l does not need to be much less than about one third of the grid

TABLE 1. Values of α for Which $\beta(\alpha, m)$ is Zero for Varying Values of m, the Exponential, Gaussian, and Whittle Correlation Functions, and With No Nugget Effect and With a 5% Nugget Effect

	Exponential		Gaussian		Whittle	
m	No Nugget	With Nugget	No Nugget	With Nugget	No Nugget	With Nugget
10	2.4	2.1	3.9	2.2	4.7	4.1
20	3.0	2.5	5.4	2.3	5.9	4.7
30	3.4	2.8	5.5	2.5	6.5	4.9
40	3.7	3.0	5.5	2.6	7.1	5.1
50	3.9	3.1	5.5	2.7	7.6	5.1
60	4.0	3.2	5.6	2.7	7.9	5.5
70	4.2	3.3	5.7	2.7	8.1	5.7
80	4.3	3.5	5.7	2.8	8.3	5.7

width L to ensure positivity of all components in $\bar{s}$. Because of its slower decay, higher values occur for the Whittle correlation. However, under appropriate normalization of the rate of decay, the results for the Whittle correlation would be essentially the same as those of the exponential model.

We conclude the section by showing in Figures 5–8 density plots of two-dimensional realizations of the exponential, spherical, Gaussian, and Whittle models. In all these simulations the parameters α and m were taken to be $\alpha = 12$ and $m = 512$; the relatively large value for α was chosen because of the slow decay of the Whittle model. A randomly located 200×200 subregion was then extracted from each 512×512 realization and displayed in Figures 5–8. Thus the realizations shown have an effective value of $\alpha \sim 4.5$. On small scales the realizations clearly show the weak local correlation of the exponential and spherical models, the very strong local correlation of the Gaussian model, and the moderate local correlation of the Whittle model. On large scales comparable to the size of the subregions all realizations are effectively uncorrelated.

The realizations were easily programmed and computed using the KHOROS image processing package and its visual programming interface on a Sun Sparc II. With these values for α and m the embeddings of the exponential, Gaussian, and Whittle models still had some negative eigenvalues, but

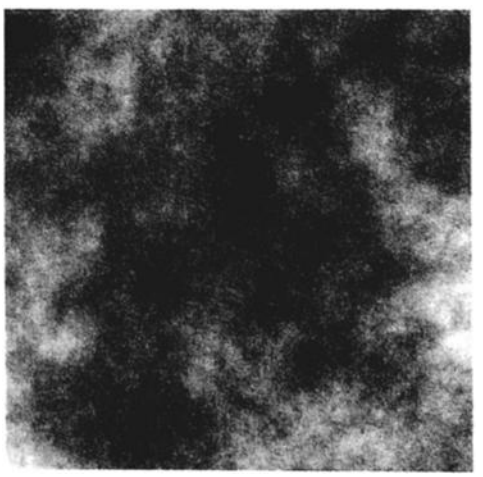

Fig. 5. Realization of a field with exponential correlation.

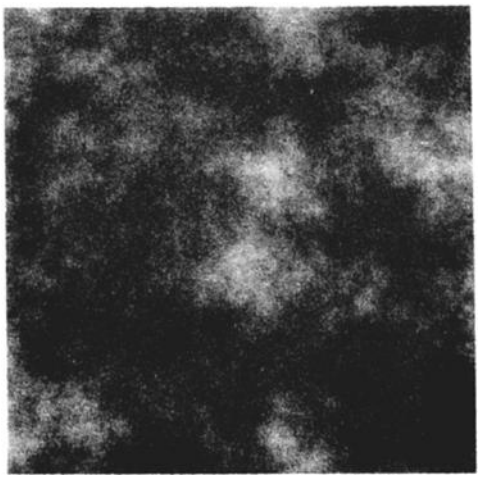

Fig. 6. Realization of a field with spherical correlation.

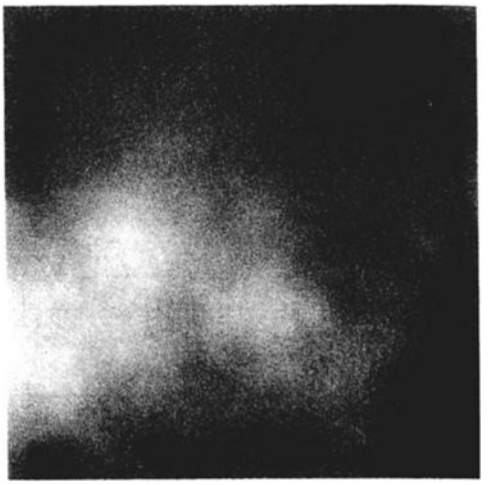

Fig. 8. Realization of a field with Whittle correlation.

these were all smaller in magnitude than machine precision and so could be set to zero without affecting the accuracy of the simulation.

6. CONCLUSIONS

The paper has presented an exact and very efficient approach to generate stationary multidimensional Gaussian stochastic simulations. The approach is based on embedding the random field Toeplitz correlation matrix in a larger matrix having circulant/block circulant structure. The set-up cost for the method is essentially the cost of the FFT of the correlation function values on the sampling grid, while computation of each simulation requires one further FFT of an appropriately weighted random vector. The only assumptions required are that (1) the sampling grid be rectangularly meshed, (2) the correlation function be invariant under translation, and (3) the embedding matrix be nonnegative definite.

While there are correlation functions for which assumption 3 is always valid, in general, to ensure a nonnegative definite embedding the sampling grid must be sufficiently large that the correlation between points on opposite sides of the grid is essentially zero. This is a very mild limitation as in most practical hydrogeological problems, the sampling grid is chosen to be large enough to ensure that the correlation function is vanishingly small at such distances. For example, this will almost always be the case when the correlation has bounded support, e.g., in the spherical and power models, as the size of the hydrogeological formation over which stochastic simulations are sought is most usually several times larger than the length scale of the correlation model. For correlations with infinite support, two-dimensional numerical experiments with the exponential, Gaussian, and Whittle models on grid of up to 80×80 nodes have shown that with inclusion of a 5% nugget effect, the ratio of the correlation length scale to the width of the grid does not need to be much less than one third to ensure nonnegativity of the embedding.

Finally, the computational requirements of the approach are comparable to those of the spectral method optimally implemented via the fast Fourier transform, yet the present approach has the advantage of generating realizations with the exactly the desired correlation structure, while the correlation of those generated by the spectral method only approximates the desired structure.

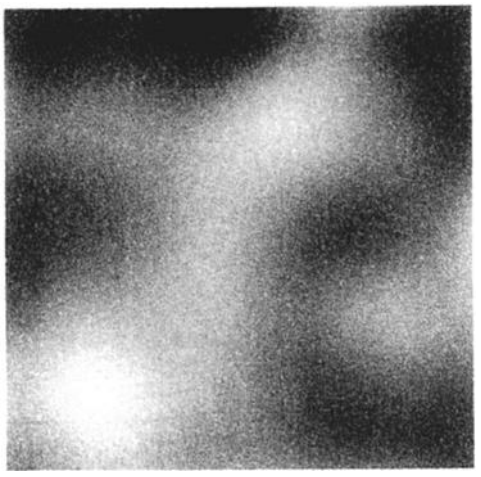

Fig. 7. Realization of a field with Gaussian correlation.

APPENDIX A

For any complex-valued quantity z let z_1 and z_2 denote its real and imaginary parts, respectively. Thus $W = W_1 + iW_2$, and $e = e_1 + ie_2$. By definition of the discrete Fourier transform matrix W, the matrices W_1 and W_2 are both symmetric. Since S is real, the eigenvalue decomposition $S = (1/2m)W\Lambda W^*$ implies that

$$S = \frac{1}{2m}(W_1\Lambda W_1 + W_2\Lambda W_2)$$

Now by definition $e = W(\Lambda/2m)^{1/2}\varepsilon$ so that

$$e_1 = W_1(\Lambda/2m)^{1/2}\varepsilon_1 - W_2(\Lambda/2m)^{1/2}\varepsilon_2 \qquad \text{(A1)}$$

$$e_2 = W_1(\Lambda/2m)^{1/2}\varepsilon_2 + W_2(\Lambda/2m)^{1/2}\varepsilon_1 \qquad \text{(A2)}$$

By construction, ε_1 and ε_2 are normal with zero means and $E[\varepsilon_i\varepsilon_j^T] = \delta_{ij}I$, $i, j = 1, 2$. Here E denotes the expectation

operator, and δ_{ij} is the Kronecker operator. Therefore from (A1) and (A2) we have

$$E[e_1 e_1^T] = \frac{1}{2m} W_1 \Lambda W_1 + \frac{1}{2m} W_2 \Lambda W_2 = S$$

$$E[e_2 e_2^T] = \frac{1}{2m} W_1 \Lambda W_1 + \frac{1}{2m} W_2 \Lambda W_2 = S$$

$$E[e_1 e_2^T] = \frac{1}{2m} W_2 \Lambda W_1 - \frac{1}{2m} W_1 \Lambda W_2 = 0$$

APPENDIX B

Let the Fourier transform $\bar{r}(x)$ of $r(x)$ be sufficiently regular (e.g., continuous) so that the Fourier transform of $\bar{r}(x)$ recovers $r(x)$. If at least one of the two functions $r(x)$ or $\bar{r}(x)$ is absolutely integrable and of bounded variation, then for any $\Delta x > 0$ the following holds true almost everywhere [*Champeney*, 1987, p. 163, theorem 15.16]:

$$\frac{1}{\Delta x} \sum_{k=-\infty}^{\infty} \bar{r}(x - k/\Delta x) = \sum_{k=-\infty}^{\infty} r(k\Delta x) \exp(2\pi i x k \Delta x) \tag{B1}$$

Because $r(x)$ is symmetric (B1) can be rewritten as

$$\frac{1}{\Delta x} \sum_{k=-\infty}^{\infty} \bar{r}(x - k/\Delta x) = r(0) + 2 \sum_{k=1}^{\infty} r(k\Delta x) \cos(2\pi x k \Delta x) \tag{B2}$$

Because $r(x)$ is a correlation function, by Bochner's theorem [*Champeney*, 1987, p. 100] $\bar{r}(x)$ is nonnegative. Therefore the right-hand side in (B2) is nonnegative for any x and positive Δx. Setting $x = j$ and $\Delta x = 1/2m$ yields the nonnegativity of (3), as by definition $\rho_k = r(k\Delta x)$.

Acknowledgment. This work was partly funded by a small Australian Research Council grant provided to one of us (C.R.D.).

REFERENCES

Barnett, S., *Matrices, Methods and Applications, Oxford Appl. Math. and Comput. Sci. Ser.*, Clarendon, Oxford, 1990.

Bartlett, M. S., *An Introduction to Stochastic Processes*, Cambridge University Press, New York, 1955.

Black, T. C., and D. L. Freyberg, Simulation of one-dimensional correlated fields using a matrix-factorization moving average approach, *Math. Geol.*, *22*(1), 39–62, 1990.

Borgman, L., M. Taheri, and R. Hagan, Three-dimensional frequency-domain simulations of geological variables, in *Geostatistics for Natural Resource Characterization*, edited by G. Verly, M. David, A. G. Journel, and A. Marechal, pp. 517–541, D. Reidel, Norwell, Mass., 1984.

Champeney, D. C., *A Handbook of Fourier Theorems*, Cambridge University Press, New York, 1987.

Davis, M. W., Production of conditional simulations via the LU triangular decomposition of the covariance matrix, *Math. Geol.*, *19*(2), 91–98, 1987.

Dietrich, C. R., Computationally efficient Cholesky factorization of a covariance matrix with block Toeplitz structure, *J. Stat. Comput. Simul.*, *45*, 203–218, 1993.

Fai Ma, M. S. W., and W. H. Mills, Correlation structuring and the statistical analysis of steadystate groundwater flow, *SIAM J. Sci. Stat. Comput.*, *8*(5), 848–867, 1987.

Jones, R. H., Fitting a stochastic partial differential equation to aquifer data, *Stoch. Hydrol. Hydraul.*, *3*, 85–96, 1989.

Journel, A. G., and C. T. Huijbregts, *Mining Geostatistics*, Academic, San Diego, Calif., 1978.

King, P. R., and P. J. Smith, Generation of correlated properties in heterogeneous porous media, *Math. Geol.*, *20*(7), 863–877, 1988.

Mantoglou, A., and J. L. Wilson, The turning bands methods for simulation of random fields using line generation by a spectral method, *Water Resour. Res.*, *18*(5), 1379–1394, 1982.

Mardia, K. V., and A. J. Watkins, On the multimodality of the likelihood in the spatial linear model, *Biometrika*, *76*(2), 289–295, 1989.

Mejia, J. M., and I. Rodriguez-Iturbe, On the synthesis of random field sampling from the spectrum: An application to the generation of hydrological spatial processes, *Water Resour. Res.*, *10*(4), 705–711, 1974.

Neuman, S. P., Universal scaling of hydraulic conductivities and dispersivities in geologic media, *Water Resour. Res.*, *26*(8), 1749–1758, 1990.

Newsam, G. N., On the asymptotic distribution of the eigenvalues of discretizations of a compact operator, in *Proceedings of the Centre for Mathematical Analysis*, vol. 17, *Special Program on Inverse Problems*, Australian National University, Canberra, 1988.

Press, W. H., B. P. Flannery, S. A. Teukolsky, and W. T. Vetterling, *Numerical Recipes: The Art of Scientific Computing*, Cambridge University Press, New York, 1986.

Shinozuka, M., and C. M. Jan, Digital simulation of random processes and its applications, *J. Sound Vibr.*, *25*(1), 111–128, 1972.

Sposito, G., W. A. Jury, and V. K. Gupta, Fundamental problems in the stochastic convection-dispersion model of solute transport in aquifers and field soils, *Water Resour. Res.*, *22*(1), 77–88, 1986.

Tompson, A. F. B., R. Ababou, and L. W. Gelhar, Implementation of the three-dimensional turning bands field generator, *Water Resour. Res.*, *25*(10), 2227–2243, 1989.

Whittle, P., On stationary processes in the plane, *Biometrika*, *41*, 434–449, 1954.

Woods, J. W., Two-dimensional discrete Markovian fields, *IEEE Trans. Inf. Theory*, *18*(2), 101–109, 1972.

Zimmerman, D. L., Computationally exploitable structure of covariance matrices and generalized covariance matrices in spatial models, *J. Stat. Comput. Simul.*, *32*, 1–15, 1989.

C. R. Dietrich, Division of Australian Environmental Sciences, Griffith University, Brisbane, Queensland 4111 Australia.

G. N. Newsam, Information Technology Division, Defense Science and Technology Organization, P. O. Box 1500, Salisbury, South Australia, 5108 Australia.

(Received October 26, 1992;
revised April 12, 1993;
accepted April 19, 1993.)